International Journal on Recent and Innovation Trends in Computing and Communication ISSN: 2321-8169
Volume: 3 Issue: 2 606 - 612

Depth Segmentation Method for Cancer Detection in Mammography Images

Parvathy S Kumar
ECE Dept
MCET
Trivandrum, Kerala
sasikumarparvathy@gmail.com

Priyanka Prabhakar
ECE Dept
Regional Centre IHRD
Trivandrum, Kerala
priya27982@gmail,.com

Aneesh R P
ECE Dept
Regional Centre IHRD
Trivandrum, Kerala
aneeshprakkulam@gmail.com

***Abstract*—** Breast cancer detection remains a subject matter of intense and also a stream that will create a path for numerous debates. Mammography has long been the mainstay of breast cancer detection and is the only screening test proven to reduce mortality. Computer-aided diagnosis (CAD) systems have the potential to assist radiologists in the early detection of cancer. Many techniques were introduced based on SVM classifier, spatial and frequency domain, active contour method, k-NN clustering method but these methods have so many disadvantages on the SNR ratio, efficiency etc. The quality of detection of cancer cells is dependent with the segmentation of the mammography image. Here a new method is proposed for segmentation. This algorithm focuses to segment the image depth wise and also coloured based segmentation is implemented. Here the feature identification and detection of malignant and benign cells are done more easily and also to increase the efficiency to detect the early stages of breast cancer through mammography images. In which the relative signal enhancement technique is also done for high dynamic range images. Markovian random function can be used in the depth segmentation. Markov Random Field (MRF) is used in mammography images. It is because this method can model intensity in homogeneities occurring in these images. This will be helpful to find the featured tumor

Keywords- *Computer aided diagnosis, KNN, Mammography, Markovian radon function SVM.*

*****

I. INTRODUCTION

Cancer is a continual multiplying of cells abnormally. The cells divide uncontrollably and will grow into adjacent tissue or unfold to distant parts of the body. Carcinoma is a number one reason for cancer deaths among women in many parts of the world. Breast cancer continues to be the foremost common diagnosed cancer among women in US. In the United States, every year, approximately, 182,000 new cases of breast cancer are diagnosed and more than 46,000 women die of it Since the causes of breast cancer still remain unknown, early detection is the key to control the breast cancer . Nowadays, mammography is considered to be the most reliable imaging modality for an early detection of breast carcinomas. If the tumor is detected at an early stage, the chances of successful treatment as well as patient survival rate will increases considerably. A mammogram is essentially distinct with four levels of the intensities such as background, breast parenchyma, fat tissue and calcifications with increasing intensity. Masses develop from the epithelial and connective tissues of breasts and their densities on mammograms blend with parenchyma patterns. Presently digital mammography is the most efficient and widely used technology for early carcinoma detection. The key diagnosing elements like masses, lesions in the digital mammograms are noisy and of very low contrast. An efficient segmentation approach to detect the early disease detection of breast cancer by enhancing the images of tumour. Most of the limitations of conventional mammography can be overcome by using digital image processing. Thus, in order to improve the correct diagnosis rate of cancer the image enhancement techniques are widely used to enhance the mammogram and assist radiologists in detecting it. Some of the efficient enhancement algorithm of digital mammograms based on wavelet analysis and modified mathematical morphology. Adopt wavelet-based level dependent thresholding algorithm and modified mathematical morphology algorithm to increase the contrast in mammograms to ease extraction of suspicious regions known as regions of interest (ROIs) are used. Several segmentation techniques are used like the gradient vector flow snake (GVF Snake) with gradient map adjustment to obtain the accurate breast boundary from the rough breast boundary and an improved multi-scale morphological gradient watershed segmentation method for automatic detection of clustered microcalcification in digitized mammograms.

II. LITERATURE REVIEW

The design and evaluation of the imaging system Clear-PEM for positron emission mammography, under development by the PEM Consortium within the framework of the Crystal Clear Collaboration at CERN, is presented in [1]. The camera consists of two compact and planar detector heads with dimensions 16.5×14.5 cm2 for breast and axilla imaging. Low-noise integrated electronics provide signal amplification and analog multiplexing based on a new data-driven architecture. The coincidence trigger and data acquisition architecture makes extensive use of pipeline processing structures and multi-event memories for high efficiency up to a data acquisition rate of one million events/s. Experimental validation of the detection techniques, namely the basic properties of the radiation sensors and the ability to measure the depth-of-interaction of the incoming photons, are presented.

In the multi-stage system [2] propose, segmentations of the breast, the nipple and the chestwall are performed, providing landmarks for the detection algorithm. Subsequently, voxel features characterizing coronal spiculation patterns, blobness, contrast, and depth are extracted. Using an ensemble of neural-network classifiers, a likelihood map indicating potential abnormality is computed. Local maxima in the likelihood map are determined and form a set of candidates in each image. These candidates are further processed in a second detection stage, which includes region segmentation,

feature extraction and a final classification. On region level, classification experiments were performed using different classifiers including an ensemble of neural networks, a support vector machine, k-nearest neighbors, a linear discriminant, and a gentle boost classifier. In [3] high specificity techniques for detecting the increased metabolic rate of breast tumours are proposed. The glucose analog FDG is known to concentrate in breast tumours rendering them easily detectable in conventional PET scans. Since PET is a relatively expensive imaging technique it has not been used routinely in the detection of breast cancer. Positron emission mammography (PEM) will provide a highly efficient high spatial resolution and low cost positron imaging system whose metabolic images are co-registered with conventional mammography. Coincidences between two BGO blocks cut into 2×2 mm squares coupled to two 7.5 cm square imaging PMTs are detected and back-projected to form real-time multiple plane images. The design is about 20 times more sensitive than a conventional multi-slice PET body scanner, so much less radio-pharmaceutical can be used, reducing the patient dose and cost per scan. Prototype detectors have been made and extensive measurements done. The device is expected to have an in-plane spatial resolution about 2 mm FWHM. Besides the application as a secondary screening tool the device may be beneficial in measuring a tumour's response to radio-therapy or chemo-therapy, as well as aiding the surgeon in optimizing the removal of malignant tissue.

In [4] detection is performed in two steps: segmentation and classification. In segmentation, regions of interest are first extracted from the images by adaptive thresholding. A further reliable segmentation is achieved by a modified Markov random field (MRF) model-based method. In classification, the MRF segmented regions are classified into suspicious and normal by a fuzzy binary decision tree based on a series of radiographic, density-related features. The detection accuracy of the algorithm was evaluated by means of a free response receiver operating characteristic curve which shows the relationship between the detection of true positive masses and the number of false positive alarms per image. The results indicated that a 90% sensitivity can be achieved in the detection of different types of masses at the expense of two falsely detected signals per image.

Neutron stimulated emission computed tomography (NSECT) is being developed [5] as a non-invasive spectroscopic imaging technique to determine element concentrations in the human body. NSECT uses a beam of fast neutrons that scatter inelastically from atomic nuclei in tissue, causing them to emit characteristic gamma photons that are detected and identified using an energy-sensitive gamma detector. By measuring the energy and number of emitted gamma photons, the system can determine the elemental composition of the target tissue. Such determination is useful in detecting several disorders in the human body that are characterized by changes in element concentration, such as breast cancer. In this paper we describe our experimental implementation of a prototype NSECT system for the diagnosis of breast cancer and present experimental results from sensitivity studies using this prototype. Results are shown from three sets of samples: (a) excised breast tissue samples with unknown element concentrations, (b) a multi-element calibration sample used for sensitivity studies, and (c) a small-animal specimen, to demonstrate detection ability from in-vivo tissue.

In [6] present an innovative imaging technology for breast cancer using gamma-ray stimulated spectroscopy based on the nuclear resonance fluorescence (NRF) technique. In NRF, a nucleus of a given isotope selectively absorbs gamma rays with energy exactly equal to one of its quantized energy states, emitting an outgoing gamma ray with energy nearly identical to that of the incident gamma ray. Due to its application of NRF, gamma-ray stimulated spectroscopy is sensitive to trace element concentration changes, which are suspected to occur at early stages of breast cancer, and therefore can be potentially used to noninvasively detect and diagnose cancer in its early stages. Using Monte-Carlo simulations designed and demonstrated an imaging system that uses gamma-ray stimulated spectroscopy for visualizing breast cancer. Show that gamma-ray stimulated spectroscopy is able to visualize breast cancer lesions based primarily on the differences in the concentrations of trace elements between diseased and healthy tissue, rather than differences in density that are crucial for X-ray mammography. In [7] a novel approach to microcalcification detection based on fuzzy logic technique is presented. Microcalcifications are first enhanced based on their brightness and nonuniformity. Then, the irrelevant breast structures are excluded by a curve detector. Finally, microcalcifications are located using an iterative threshold selection method. The shapes of microcalcifications are reconstructed and the isolated pixels are removed by employing the mathematical morphology technique. The essential idea of the proposed approach is to apply a fuzzified image of a mammogram to locate the suspicious regions and to interact the fuzzified image with the original image to preserve fidelity.

In [8] a novel algorithm to detect suspicious lesions in mammograms is developed. The algorithm utilizes the combination of adaptive global thresholding segmentation and adaptive local thresholding segmentation on a multiresolution representation of the original mammogram. In [9] developed a biologically derived mammographycompanding (BDMC) algorithm for compression, expansion, and enhancement of mammograms, in a fully automatic way. The BDMC is comprised of two main processing stages: 1) preliminary processing operations which include standardization of the intensity range and expansion of the intensities which belong to the low intensity range. 2) Adaptively companding the HDR range by integrating multiscale contrast measures.

III. PROPOSED METHOD

With increasing use of Computed topography (CT) and Magnetic resonance (MR) imaging for diagnosing, treatment and clinical studies, it has become nearly mandatory to use computers to help radiological experts in clinical diagnosis, treatment coming up with. Reliable algorithms are required for the delineation of anatomical structures and other regions of interest (ROI).The techniques obtainable for segmentation of medical images are specific to applications, imaging modality and kind of body part to be studied. For example necessities of brain segmentation are different from those of thorax. The proposed method is based on a segmentation technique in MRI images as well as high dynamic range MRI images mainly focused on the breast cancer detection. and also for the detection of benign and as well as malignant tumours. Usually the segmentation based on the lesions are done before the analysis and enhancement so here propose a technique based

on the depth segmentation and then detect the carcinoma tumour in the mammography images. And this can be proposed based on the markovian or laplacian depth based segmentation can be done and then finally enhance using a median filter, which is nothing but the denoising of unwanted speckles and noises. The artifacts, that have an effect on the brain image, are such that the different partial volume effect is more prominent in brain while in the thorax region it is motion artifact is more prominent.

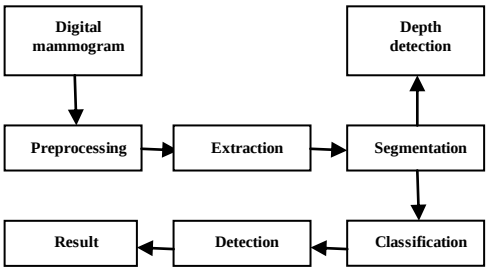

Figure 1. Basic Block Diagram

A. Preprocessing

The input images are of the type high dynamic range mammography images. These images were antecendly investigated and labeled by an expert radiologist based on technical expertise and diagnostic test. The dataset is chosen as a result of the varied cases. The dataset consists of 322 mammograms of right and left breast, from 161 patients, wherever fifty one were diagnosed as malignant, sixty four as benign and 207 as normal. The abnormalities are classified as microcalcification, ill-defined mass, speculated mass, architectural distortion, circumscribed mass and asymmetry .In this study about 322 mammogram images were chosen. The original mammograms are 409 x 700pixels, and almost 50% of the image comprised of the background with a lot of noise. Within the planned CAD system, microcalcifications aren't thought-about; solely circumscribed mass, spiculated mass, architectural distortion, ill-defined mass, and imbalances are thought of. The preprocessing part of digital mammograms refers to the sweetening of mammograms intensity and distinction manipulation, effect of noise reduction, unwanted background removal, edge sharpening and filtering.

B. Watershed transform for segmentation

Instead of performing on an image itself, this system is usually applied on its gradient image. In this case, each object is distinguished from the background by its up-lifted edges. M_1, M_2, …, M_R as the sets of the coordinates of the points in the regional minima of an (gradient) image g(x,y), and $C(M_i)$ as the coordinates of the points in the catchment basin associated with regional minimum M_i.The minimum and maximum gray levels of g(x,y) are denoted as *min* and *max* Denote T[n] as the set of coordinates (s,t) for which g(s,t) < n. Flood the topography in integer flood increments from n=*min*+1 to n=*max*+1 .At each flooding, the topography is viewed as a binary image.Denotes $C_n(M_i)$ as the set of coordinates of points in the catchment basin associated with minimum M_i at flooding stage n.

$C_n(M_i)= C(M_i) \cap T[n]$
$C_n(M_i)=\subseteq T[n]$

C[n] is defined as the union of flooded catchment basin portions at stage n.

$$C[n]=\bigcup_{i=1}^{R} C_n(M_i) \text{ and } C[\max+1]=\bigcup_{i=1}^{R} C(M_i)$$

Let C[min+1]=T[min+1].At each step n, assume C[n-1] has been constructed. The goal is to obtain C[n] from C[n1].Denote Q[n] as the set of connected components in T[n]. For each q∈Q[n], there are three possibilities:

- q ∩ C[n-1] is empty (q1) A new minimum is encountered as the q is incorporated into C[n-1] to form C[n].
- q ∩ C[n-1] contains one connected component of C[n-1] (q2).q is incorporated into C[n-1] to form C[n].
- q ∩ C[n-1] contains more than one connected components of C[n-1] (q_3).

A ridge separating two or more catchment basins has been encountered. A dam has to be built within q to prevent overflow between the catchment basins Repeat the procedure until n=max+1.Final equation that is used as the watershed transform is

$$\boldsymbol{W_{shed}}\,(\boldsymbol{f}) = \boldsymbol{D} \cap (\cup_{i\in I}\ \boldsymbol{CB}(\boldsymbol{m_i}))^{\boldsymbol{c}}$$

The steps involved in watershed segmentation are :

- Gradient magnitude of image is detected and watershed transform is applied; fig(c,d)
- Opening-closing by reconstruction of the image is determined; fig(e)
- Regional maxima of opening and closing by reconstruction.
- Thresholding is done.
- Object boundaries are marked; fig(f)
- Colored watershed label matrix is obtained through which the tumour is segmented from the input image.

C. Kinetic Parameters

Adequate diagnosis of ductal carcinoma in mammography images could lead to efficacious treatment. Attributable to the actual fact that DCIS lesions will reach to invasive carcinomas and that the sensitivity of the standard examination – mammography – is between 70 and 80%, use of a lot more sensitive diagnostic tool was required. In the detection of DCIS the contrast enhanced magnetic resonance imaging (CE-MRI) has the sensitivity up to 96%. Morphological features and kinetic parameters were evaluated to outline the foremost regular kinetic, morphological and morpho-kinetic patterns on MRI assessment of breast ductal carcinoma in situ (DCIS). DCIS appeared most frequently as non-mass-like lesions (12 lesions, 52.17%). The differences in the frequency of lesion types were statistically significant (P<0.05). The morphological patterns were detected are morphologic features, linear or branching enhancement, focal mass-like enhancement, segmental enhancement, segmental enhancement in triangular shape, diffuse enhancement, regional heterogeneous enhancement in one quadrant not

conforming to duct distribution and dotted or granular type of enhancement with patchy distribution. The distinction within the frequency of the planned patterns was statistically important (P>0.05). There have been eight lesions with mass improvement, and 6 with segmental lesions: regional and triangular. There was no statistically important distinction within the frequency of enhancement curve varieties (P>0.05). There was no significant difference in the frequency of morpho-kinetic patterns. The objective was to analyze the morphology and kinetic features of DCIS to define the most frequent morphologic and kinetic patterns.By this we obtain a graph that shows the kinetic parameters based on position.

The analysis based on the intensity is also made so that the exact mass lesion is identified for further treatment. The risk of malignancy depends on the kinetic pattern, ranging from 6% in type I and 64% in type II to 87% in type III . Rapid uptake is most frequently related to DCIS within the initial section, whereas all 3 sorts of curves are seen within the delayed section, of that the plateau kind is that the commonest. The approaches for image segmentation mentioned here will be graded on the idea of pertinency, suitableness, performance, and process computational cost. Segmentation techniques supported grey level techniques like thresholding, and region based mostly techniques are the only techniques and notice restricted applications. A range of various neural network-based algorithms also are available for texture-based segmentation and classification having sensible accuracy. However, most of those neural network-based algorithms need intensive oversight and training and their performance depends upon the training methodology and knowledge utilized in training. Finally, it's desired from medical image segmentation and classification algorithms that they have to have the subsequent features like accuracy, repeatability, reliability, least dependency on the operator and robustness etc. A proposed method is introduced to increase clarity based on the depth segmentation approach in mammography images for the early detection of breast cancer.

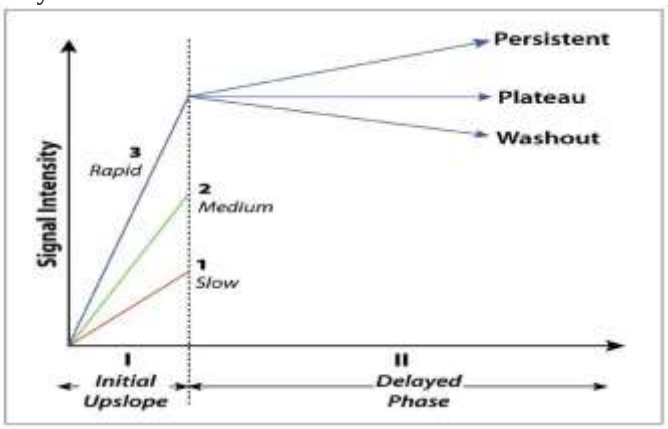

Figure 2. Enhancement kinetics curves seen with mammography images

D. Markov Random Function

Consider a multivariable random vector f = $[f_1,\ldots,f_m]^T$, whose component,fi; i = 1,…,m; represents the discriminative score of ith gene (protein) between two phenotypes[10]. The phenotypes are such as early recurrence and late recurrence respectively. In a PPI network, S represents a sequence set of m genes in a network, and Ni represents the connected neighbours of gene i. A 1-vertex clique C 1 as the set of S and a 2-vertex clique C 2 on Ni and S is defined as:

$$\boldsymbol{C_2 = \{\{\iota, \dot{\iota}'\}\, \iota' \in N_i, \iota \in S\}}$$

The random variable vector f is the Markov random field on *S* with respect to *Ni* and subject to the following conditions:

$$\boldsymbol{P(f) > 0, \forall\, f \in F\}}$$

$$\boldsymbol{P(f_i, f_{s-\{i\}}) = P(f_i, f_{N_i})}$$

Cellular Neural/Nonlinear Networks Universal Machine (CNN-UM), which is a new imageprocessing tool, containing thousands of cells with analog dynamics, local memories and processing units. The ModiRed Metropolis Dynamics (MMD) optimization method can be implemented into the raw analog architecture of the CNN-UM. We can introduce the whole pseudo-stochastic segmentation process in the CNN architecture using 8 memories/cell. We use simple arithmetic functions (addition, multiplication), equality-test between neighboring pixels and very simple nonlinear output functions (step, jigsaw). With this architecture, the proposed VLSI CNN chip can execute a pseudo-stochastic relaxation algorithm of about 100 iterations in about 100 ms.In the suggested solution the segmentation is unsupervised, where a pixel-level statistical estimation model is used. A Gaussian mixture model is a probabilistic model that assumes all the data points are generated from a mixture of a finite number of Gaussian distributions with unknown parameters. Suppose X = $\{x_1, x_2 \ldots, x_N\}$ is a random observation data set. x_i is a d-dimensional random variable. $pi(x|\theta i)$is the corresponding probability density function, in which $x \in Rd$ is the value of x_i and θ_i is the parameter. In segmentation application, the FGM assumes that the entire image can be expressed as overlaps of Gaussian distributions of its features. Suppose that xi is the observed intensity of pixel. And let L, I and γ denote the sets of tissue class L= {lesion, non-lesion}, pixel index I = {1,2, ..., N}, and model parameters $\gamma = \{\theta l \mid l \in L\}$ respectively. For every l ∈ L and i ∈ I, $l_i \in L$

$$P(xi|l) = f(xi; \theta l)$$

Finite Gaussian Model is defined by mean μ_l and variance σ_l as follows:

$$f(x_i; \theta_l) = \frac{1}{\sqrt{2\pi\sigma_l^2}} \exp\left(-\frac{(x_i - \mu_l)^2}{2\sigma_l^2}\right)$$

It is a mathematically simple model and can be computed efficiently. But one of the limitations is not considering spatial information. This method only uses the intensity histogram for segmentation, and therefore, it is sensitive to noise and other artifacts.

The Markov Random Field is proposed to overcome this weakness.MRF adds the term $P(l)$ to Equation 3, and solves the segmentation problem with maximizing.$P(l)$ Indicates the prior probability distribution of class tissue *l*.

$$\boldsymbol{\hat{l} = l^{argmax P(l/x)} = l^{argmax P(x/l) P(l)}}$$

In other words, the only difference between FGM and MRF model lies in whether the spatial constraint is encoded. To estimate the *P*(*l*), based on the Hammersley-Clifford theorem we can write:

$$\boldsymbol{P(l) = Z^{-1}\, exp\big(-U(x)\big), and U(x) = \sum_{c \epsilon C} V(x)_c}$$

Where *Z* is a normalizing constant, *U*(*x*) is the energy function, and *Vc* denotes a clique potential.

The second criterion is the Markov property of a random field, wherever the probability of a explicit configuration at gene *i* is statistically independent of the configurations of all other genes (j ε S) given the configuration of Ni. Specifying the joint probability P(f) for a Markov random field is usually refractory. The equivalence between MRF and Gibbs distributions provides an alternative means to specify P(f) using Gibbs distribution. The attainable configuration f of a set of random variable vector F obeys a Gibbs distribution if the joint distribution takes the following form:

$$\mathrm{P}(\boldsymbol{f}) = \frac{\mathbf{1}}{\boldsymbol{W}} \times \boldsymbol{e}^{-\frac{U(f)}{T}}$$

where *W* is a normalizing constant and *U*(**f**) is given by

$$\boldsymbol{U(f) = \sum_{c \epsilon C} V_C\,(f)}$$

$$\boldsymbol{C = C_1 \cup C_2}$$

Note that C is the union set of 1-vertex clique C_1 and 2-vertex clique C_2 where U(f) is the prior energy which is given by a sum of clique potentials Vc (f) over all cliques. Vc (f) represents the potential on clique c, and the value of Vc (f) depends on the local configuration on the clique c; for the mathematical definition of Vc (f). Here clique potentials allow the modelling of knowledge (a priori) about the contextual interactions between genes at neighboring sites. We usually assign zero potential to all cliques of size >2. The energy U(f) corresponds to the probability of that configuration. The parameter T, typically referred to as temperature will control the sharpness of the distribution. The calculation of the partition function W is a formidable task, even for comparatively small problems. It is needless to calculate W in our maximum a posterior (MAP) framework because it is a normalization constant.

Denote the observed discriminative scores of genes between two phenotypes as $Z = \{Z_1,\ldots,Z_m\}$. Here, we define Z_i as the *Z*-score of its corresponding *P*-value P_i using $Z_i = \Phi^{-1}(1\text{-}P_i)$ Where Φ^{-1} is the inverse normal cumulative density function. *P*-value can be obtained by statistical methods for hypothesis testing. The observed discriminative score is a result of the addition of independent zero mean Gaussian noise to the underlying discriminative score Z = f+e, e ~ N(0,1). One possible estimate of the underlying discriminative score **f** is the MAP estimate $\hat{f}$ that maximizes the likelihood of posterior probability (log P(f | Z)). Considering Bayes' rules and a Gibbs distribution, the MAP estimate f minimizes the following posterior potential function. The first term in the posterior potential function is the prior potential given by:

$$\boldsymbol{U(f) = \sum_{i \in S} V_i\,(f_i) + \sum_{i \in S} \sum_{i \in S} V_2\,(f_i, f_{i'})}$$

$$\boldsymbol{= \frac{-1}{m} \sum_{i \in S} f_i + \frac{\lambda}{k} \sum_{(i,i') \in E} \left(\frac{f_i}{\sqrt{d_i}} - \frac{f_{i'}}{\sqrt{d_{i'}}}\right)^2}$$

where d_i is the degree of gene *i* in the PPI network (defined by the number of edges connected to gene *i*), *k* is the number of interactions (or edges) and λ is a trade-off parameter. The first term in equation is the average discriminative score in a subnetwork and the second term in equation imposes the smoothness across the subnetwork while placing more weights on the genes with large degrees. The posterior potential function is normalized by the number of genes and edges in the subnetwork. Henceforth, this function is independent of the subnetwork size. The second term in the posterior potential function is the likelihood potential given by:

$$\boldsymbol{U(Z/f) = \frac{\gamma}{m} \sum_{i \in S} (Z_i - f_i)^2 / 2}$$

where γ is a known as the trade-off parameter. The potential represents the average square of difference between the observed and underlying discriminative scores, considering the assumption of a Gaussian distribution of the noise signal with 0 mean and 1 SD. The default value for λ and γ is as set 1. Thus, we can define the subnetwork score as the negative posterior potential function that takes into account the dependency among the genes of a subnetwork as[10]:

$$\boldsymbol{Netscore\,(G) = -U(\hat{f}/Z)}$$

$$\boldsymbol{G = \frac{1}{m} \sum_{i \in S} \hat{f_i} - \frac{\lambda}{k} \sum_{(i,i') \in E} \left(\frac{\hat{f_i}}{\sqrt{d_i}} - \frac{\lambda}{m} \sum_{i \in S} (Z_i - \hat{f_i})^2 / 2\right)}$$

IV. RESULTS

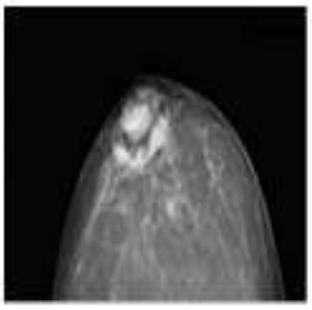

Figure 1. a. Input image. b. Edged image

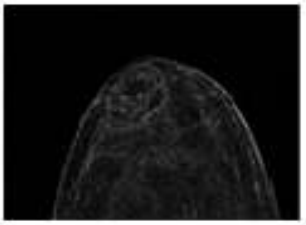

Figure 2. c. Gradient image d. Watershed Transform

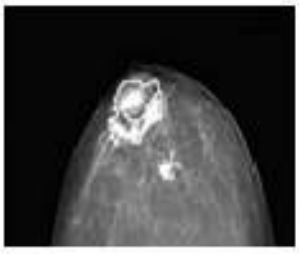

Figure 3. e. Regional maxima f. Object marking

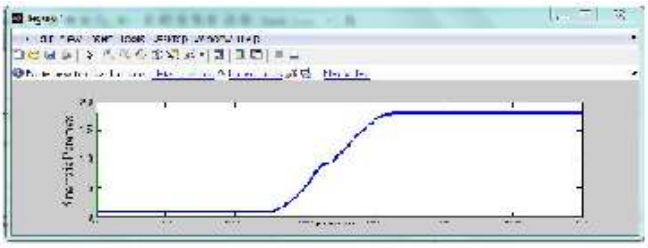

Figure 4. g. Kinetic parameter response

Figure 5. h. Kinetic Intensity Response

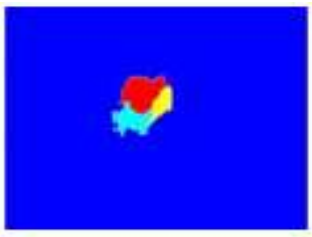

Figure 6. i. Coloured watershed Label matrix

TABLE I. COMPARISON OF RESULT

Method	Accuracy (%)
Proposed Method	96.98
Discriminant Analysis	87.11
ANN	95.45
Decision Tree	92.89
Logistic Regression	93.78
SVM	95.79
KNN	94.78
Naïve Bayes	95.19

Here it is seen that the extracted tumour based on the watershed segmentation in which the image that showing the regional maxima is then implemented based on the kinetic parameter as it is plotted with the position gives that the tumour part shows a increase in washout parameters.

V. CONCLUSION

A general introduction of the potential and challenges of breast carcinoma detection was given. With digital imaging taking part in an progressively outstanding role within the diagnosis and treatment of diseases, the matter of extracting clinically useful data has become vital. For instance, mammography facilitates to outline the character and extent of diseases, aiding the diagnosis and treatment. Therefore, segmentation of those features becomes a key challenge for correct analysis, visualisation and quantitative comparison. This has been the most focus of this treatise, i.e., segmentation of normal and abnormal features. From each range and variety of algorithms used for carcinoma detection it had been clear that there's no gold customary that solves entire downside. It's been dedicated to the preprocessing and outline of mammogram databases wont to appraise the strategies. a number of the pictures were discarded by doctors before the identification. However such pictures were images within the database to ascertain the enclosed of the developed system. Images that suffered from non uniform illumination and poor contrast were subjected to preprocessing before they are subjected to segmentation. . This algorithm focuses to segment the image depth wise. Here the identification of malignant and benign cells is done more easily and also to increase the efficiency of the mammogram images. In which the relative signal enhancement technique is also done for high dynamic range images. Markovian random function can be used in the depth segmentation. For every image within the database the region of interest is well defined. Thus validation prevents over fitting and goes how to make sure the relevance of the results to a wider set of images.

REFERENCES

[1] M. C. Abreu, Aguiar J.D., Almeida F.G. and Almeida P "Design and evaluation of the Clear-PEM scanner for positron emission mammography", IEEE Trans. Nucl. Sci. vol 53, number 1, pp.71-77, 2006

[2] Tao Tan , Platel B,. Mus R., Tabar L. and Mann, R.M. , "Computer-Aided Detection of Cancer in Automated 3-D Breast Ultrasound", IEEE Trans. Medical Imaging. vol 32, issue 9, pp.1698-1708, May 2013

[3] C. J. Thompson et al., "Positron Emission Mammography (PEM): a promising technique to detect breast cancer", IEEE Trans. Nucl. Sci. vol. 42, pp.1012-1017, 1995.

[4] Li H.D, Kallergi M, Clarke L.P, Jain V.K and Clark R.A , "Markov random field for tumor detection in digital mammography " IEEE Trans. on Medical Imaging Vol 14, Issue 3, 565:576–958, Sep. 1995

[5] Kapadia A.J, Sharma A.C, Tourassi G.D, Bender J.E, Howell C.R, Crowell A.S and Kiser M.R "Neutron Stimulated Emission Computed Tomography for Diagnosis of Breast Cancer " IEEE Trans. on Medical Imaging Vol 55, Issue 1, pp.501–509, 2008

[6] Lakshmanan M.N, Harrawood B.P, Agasthya G.A and Kapadia A.J, "Simulations of Breast Cancer Imaging Using Gamma-Ray

Stimulated Emission Computed Tomographyr ” IEEE Trans. on Medical Imaging Vol 33, Issue 2, pp.546–555, 2014

[7] Heng-Da Cheng, Yui Man Lui and Freimanis R.I, “A novel approach to microcalcification detection using fuzzy logic technique ” IEEE Trans. on Medical Imaging Vol 17, Issue 3, pp.442-450, June 1998

[8] Kanelovitch L, Itzchak Y, Rundstein Aand Sklair M, “Biologically Derived Companding Algorithm for High Dynamic Range Mammography Images” , IEEE Trans. on Biomedical Engineering Vol 60, Issue 8, pp.2253-2261, 2013

[9] Kai Hu, Xieping Gao and Fei Li, “Detection of Suspicious Lesions by Adaptive Thresholding Based on Multiresolution Analysis in Mammograms ” , IEEE Trans. on Instrumentation and Measurement, Vol 60, Issue 2, pp.462-472, 2011

[10] Chen L, Xuan J, Gu J, Wang Y, Zhang Z, Wang TL and Shih IeM., “Integrative Network Analysis To Identify Aberrant Pathway Networks In Ovarian Cancer ” , Pac Symp Biocomput. 2012:31-42.